ELECTRICAL SIZING OF

PARTICLES IN SUSPENSIONS

## III. RIGID SPHEROIDS AND RED BLOOD CELLS

N. B. GROVER, J. NAAMAN, S. BEN-SASSON, *and* F. DOLJANSKI

From the Department of Experimental Medicine and Cancer Research, The Hebrew University–Hadassah Medical School, Jerusalem, Israel

ABSTRACT   The processes involved during the passage of a suspended particle through a small cylindrical orifice across which exists an electric field are investigated experimentally for an approximate prolate spheroid in the form of two tangent, rigid spheres (ragweed pollen particles) and for fresh, human red blood cells. Oscillograms of current pulses produced by both types of particles are presented and discussed in terms of particle shape and orientation and the effects of the hydrodynamic field. It is concluded that all the particles enter the orifice with their major axes aligned parallel to the orifice axis (electric field), but that during their passage some are rotated by the hydrodynamic field. Cells with their equatorial plane perpendicular to a radius of the orifice change their orientation with respect to the electric field as they are rotated, the others do not; only in the former case is there any deformation. It is shown that the bimodal or skewed size distributions can be explained on this basis, and that size (shape factor × volume) is actually a normally distributed variable ($P > 95\%$). The average size of samples from 10 healthy adults was found to be 102.7 μ^3 with a coefficient of variation of 1.8%. For a volume of 87 μ^3, this corresponds to a shape factor of 1.18, an axial ratio (assuming a perfect oblate spheroid) of 0.26, and an equivalent major axis of 8.6 μ. The effect of high electric fields on red cell size distributions is mentioned.

INTRODUCTION

The size of human red blood cells is often a reflection of the physiological and pathological state of their donor and so has been of considerable interest for some time (1). The advent of the Coulter transducer (Coulter Electronics, Industrial Div., Hialeah, Fla.) has made possible the rapid determination of cell size distributions on large samples. Usually these distributions are reported as being positively skewed (2–19), although the experimental conditions can be chosen in such a way that the skew increases until a distinct bimodal distribution is obtained (6–15, 20–23) or decreases until it disappears altogether and a perfectly symmetrical distribution remains (14–21). Several investigators (3–9, 19–23) have accepted the bimodal
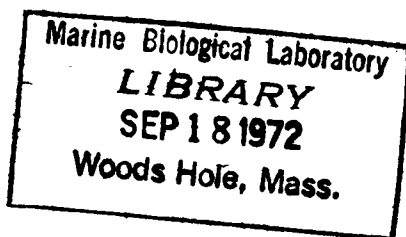
(or skewed) distribution as reflecting the actual volume distribution of red blood cells, others (10, 11) have felt the need to invoke additional physical properties in order to explain this lack of symmetry; some (2, 12–18) claim it to be an artifact of the measuring system. In the present paper, we shall investigate the origins of the skewed distribution, show that it is indeed an artifact of the transducer, and describe procedures for determining the true distribution; we shall also present evidence that the size of human red blood cells is normally distributed (gaussian).

Theoretical expressions describing the processes involved during the passage of a suspended particle through a small cylindrical orifice across which exists an electric field have been presented in the first paper of this series (24); experimental verification for the case of rigid spheres was provided in the second (25), together with a detailed description of the measuring system. In those articles it was shown that under appropriate conditions the *size* of a nonconducting particle of volume v, when determined electrically, is equal to γv, where γ is a factor that depends on the shape of the particle and on its orientation in the electric field. Since shape is affected by distortion and orientation by rotation, the electrical size of a particle will in general depend on many factors other than its geometry; in order to try to differentiate among them, a preliminary series of experiments was carried out using rigid spheroids with well-defined shapes and volumes: ragweed pollen particle doublets.

RAGWEED DOUBLETS

By decreasing the sonication time in the previous preparation procedure (25) from 40 to 30 sec, suspensions of ragweed pollen particles can be obtained consisting of about 85% single spheres and 15% doublets; the concentration of higher aggregates is very small. Since the formation of doublets is nonselective (this is easily established by increasing the sonication time, which breaks up the doublets, and observing that the mean volume of the singlets remains unchanged), their mean volume is precisely twice that of the singlets; because of the small spread (25) in singlet diameters [coefficient of variation (c.v.) $< 5\%$], all doublet particles have practically identical shapes. In addition the rigidity of ragweed precludes distortion, and any slippage of one sphere relative to the other can be looked upon as rotation at constant shape and volume.

The shape factor γ of a spheroid of given axial ratio is a simple function of its orientation ψ, obeying a relationship first derived in connection with the thermal conductivity of anisotropic solids (26) which, in the notation of reference 24, takes the form $\gamma(\psi) = \gamma \cos^2 \psi + \gamma' \sin^2 \psi$. In order to simplify the discussion when comparing prolates and oblates, we now introduce $\gamma(a)$ and $\gamma(b)$ as the minimum and maximum values of γ, respectively, for both types of spheroids. The above expression then becomes $\gamma = \gamma(a) \cos^2 \theta + \gamma(b) \sin^2 \theta$, where for prolates θ is measured between the major axis of the spheroid and the electric field and for oblates between the minor axis and a plane perpendicular to the field. [For a sphere $\gamma = \gamma(a) =$
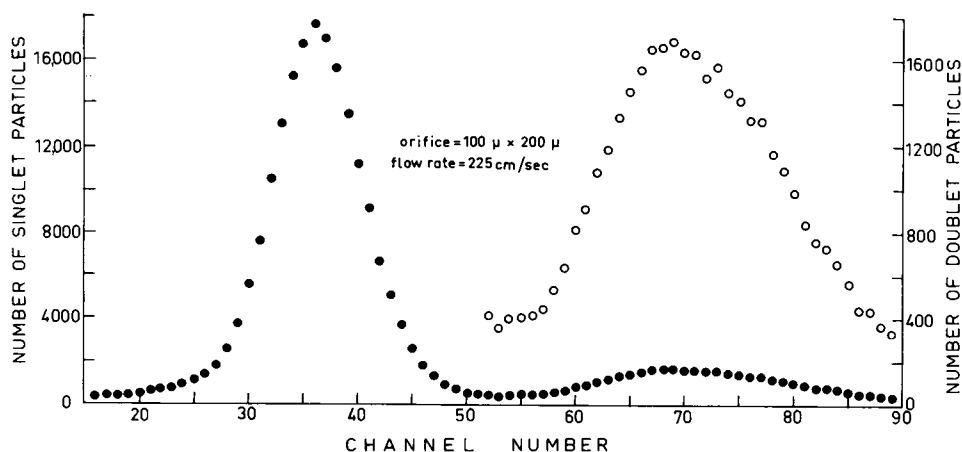
FIGURE 1 Size distribution of ragweed pollen particles (closed circles, left-hand scale). The doublet distribution is replotted on an expanded (×10) vertical scale (open circles, right-hand scale).

$\gamma(b)$ = 1.5.] Since the shape of a doublet is roughly like that of an ellipsoid with axial ratios 2:1:1, $\gamma(a)$ can be expected (24) to be about 1.2 and $\gamma(b)$ about 1.7.

When we attempt to measure the size distribution of such a ragweed suspension (25), we obtain the plot shown in Fig. 1. Here two distinct populations are apparent, the one on the left, which is narrow and symmetrical and represents the large singlet population, and the one on the right, which represents the doublets and has a pronounced positive skew. (Negative skew, which is less common and occurs when the mean size of a population lies to the left of its mode, can be obtained by altering the orifice dimensions or the flow rate and is illustrated in Fig. 4 b.)

In the remaining paragraphs of the present section we show that the doublet size distribution is actually a superposition of two distinct distributions, which we call α and β, and in the following section we apply this result to an analysis of red cell size distributions. Before attempting to interpret a size distribution like that shown in Fig. 1, it is necessary to turn to the separate events that together give rise to the distribution. Thus by observing the current pulses produced by individual doublets as they are pumped through the orifice, one can determine their size at various positions within the orifice and so study the effects of orientation and rotation directly. Several representative pulses obtained with an orifice 100 μ in diameter by 200 μ in length (nominal dimensions) are shown in Fig. 2.

Most of the pulses are of course produced by the large singlet population, and in each frame a singlet pulse has been superimposed for purposes of comparison. These pulses give rise to the singlet distribution of Fig. 1 and were described in detail previously (24). The higher pulses in Fig. 2 are caused by the doublet particles and are of two distinct types: those (type B) that exhibit a peak at some point during the passage of the particle (frames b–d), and those (type A) that remain flat throughout
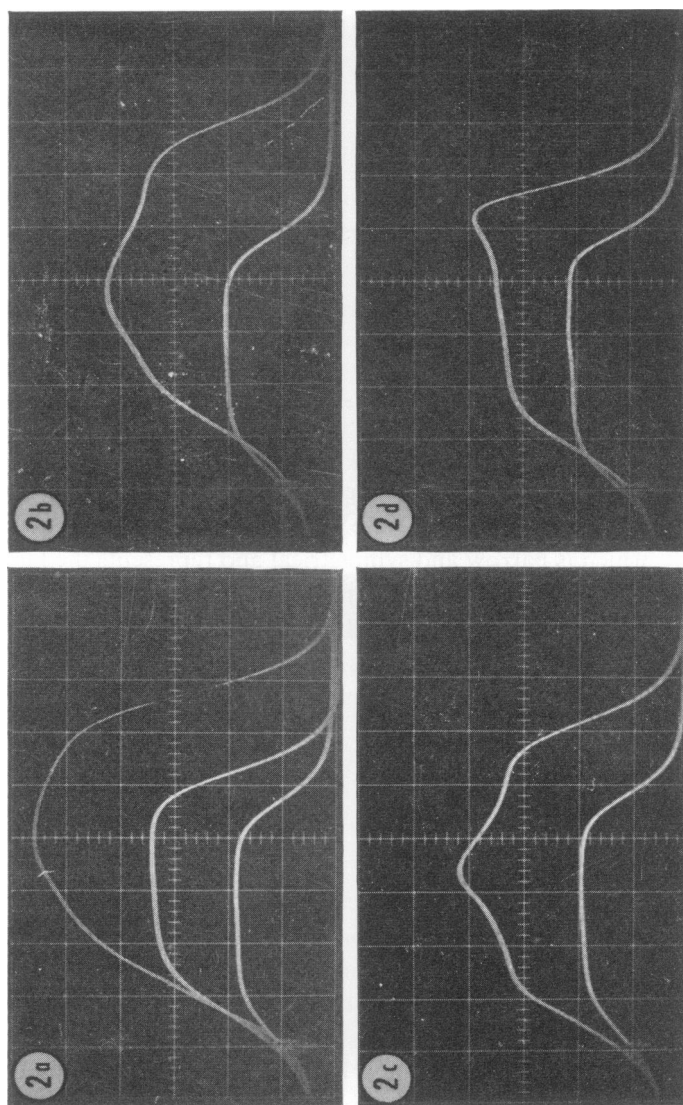
FIGURE 2 Oscillograms of pulse shapes of singlet and doublet ragweed pollen particles in an orifice 100 × 200 μ. Flow rate, 450 cm/sec; sweep, 7.7 μsec/division.

(frame *a*, which includes a rare triplet pulse). It is obvious that a suitable combination of such doublet pulses will give rise to a size distribution like that shown in Fig. 1 for the doublet population, and that by increasing the proportion of type *B* pulses, the mode can be shifted to the right and a negatively skewed distribution obtained.

The relative spread in the amplitudes of the type *A* pulses is no greater than that of the singlet pulses, implying that not only do those particles that give rise to type *A* pulses not rotate during their passage through the orifice but that they actually enter the orifice all similarly oriented. This is a fortunate result and quite unexpected. From symmetry considerations the most likely orientation is that with the major axis either parallel or perpendicular to the orifice axis; from energy considerations, the former (minimum shape factor) is to be preferred. It should perhaps be mentioned that among the thousands of type *B* pulses that we have observed, never have we seen a peak drop below the level of the rest of the pulse. This, and the fact that the pulse amplitude before and after the peak is essentially identical with that of the flat (type *A*) pulses, indicates that the major axes of the doublets are all initially parallel to the axis of the orifice, but that some of the doublets undergo a rotation during their passage. That this is indeed so can be established (see below) by calculating the shape factor corresponding to the mean pulse amplitude and comparing it with the theoretical values at different orientations.

The most obvious feature of type *B* pulses is their long duration and the fact that the wider the pulse, the earlier its peak occurs (Fig. 2). Before we can propose an explanation for the rotation of the doublets and the shape of the resulting pulses, it is necessary to recall briefly the nature of the hydrodynamic field within the orifice. Under the assumption that the fluid velocity in the axial direction is uniform across the entrance of the orifice, we have already shown (24) that the width of this region of uniform flow, the core region, is a maximum at the entrance and decreases slowly downstream because of the finite viscosity of the fluid. This is shown in Fig. 3 for each of the orifices and flow rates used. Thus a particle traversing the orifice parallel to the axis will leave the core region sooner the farther its path lies from the axis; if it is near enough to the axis, it will not leave the core region at all. Since the sooner a particle leaves the core region the longer it spends in the boundary layer, where the flow is retarded, the correlation between the duration of a pulse and the position of its peak that is so evident in Fig. 2 is readily explained by assuming that a type *B* pulse is caused by a sudden rotation of the doublet particle as it leaves this region and enters the boundary layer.

It should be pointed out that there is no direct connection between type *B* pulses, a hydrodynamic effect, and the M-shaped pulses described previously (24) and which are caused by the nonuniform electric field; these latter have been eliminated in the present paper by suitable adjustment of the gating circuits (25).

Clearly the mean size obtained from the doublet distribution of Fig. 1 reflects an average shape factor whose actual value will depend on the proportion of doublets
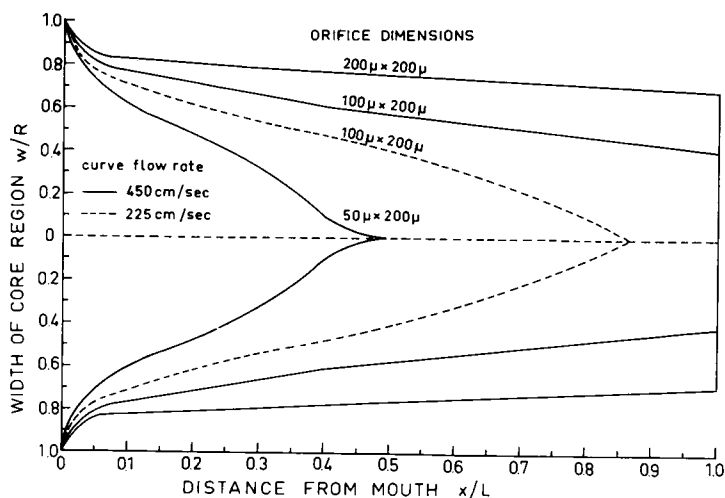
FIGURE 3 Contour of width of core region w in units of orifice radius R as a function of distance from mouth of orifice x in units of orifice length L. Orifice dimensions and flow rates are indicated.

that rotate and their degree of rotation. This γ can be calculated directly even from uncalibrated output data: the ratio of mean doublet channel (or window or threshold) to mean singlet channel is just $2\gamma v/1.5v$ and is completely independent of the experimental parameters of the measuring system (current, amplification, orifice volume) provided only that it is linear.

The relative proportion of type A and type B pulses, and hence γ, can be changed by altering the hydrodynamic field. (The electric field can easily be shown to have no effect.) Thus a decrease in the radius of the orifice while keeping the length fixed (or increasing the length and keeping the radius fixed) increases the chance of a particle entering the boundary layer before it leaves the orifice, and the number of type B pulses rises, and with it γ. The effect of decreasing the flow rate is somewhat more involved. On the one hand, it will increase the number of doublets that leave the core region, as a decrease in radius does; on the other hand, the resulting lowering of the gradient across the edge of the boundary layer may decrease γ by decreasing the degree of rotation of the doublets that give rise to the type B pulses. For a particular orifice, the combined effect on γ will depend on particle geometry; in general we can expect that the greater the eccentricity of a spheroid the more difficult its rotation becomes, prolates being easier to rotate than oblates. A larger decrease in the flow rate can result in the hydrodynamic forces being insufficient to align the spheroid axes completely with the orifice axis on entrance, and in such a case γ would actually increase.

Depending on the orifice dimensions and on the flow rate, therefore, one would expect γ to vary from somewhat above its minimum value $\gamma(a)$ of 1.2 when condi-
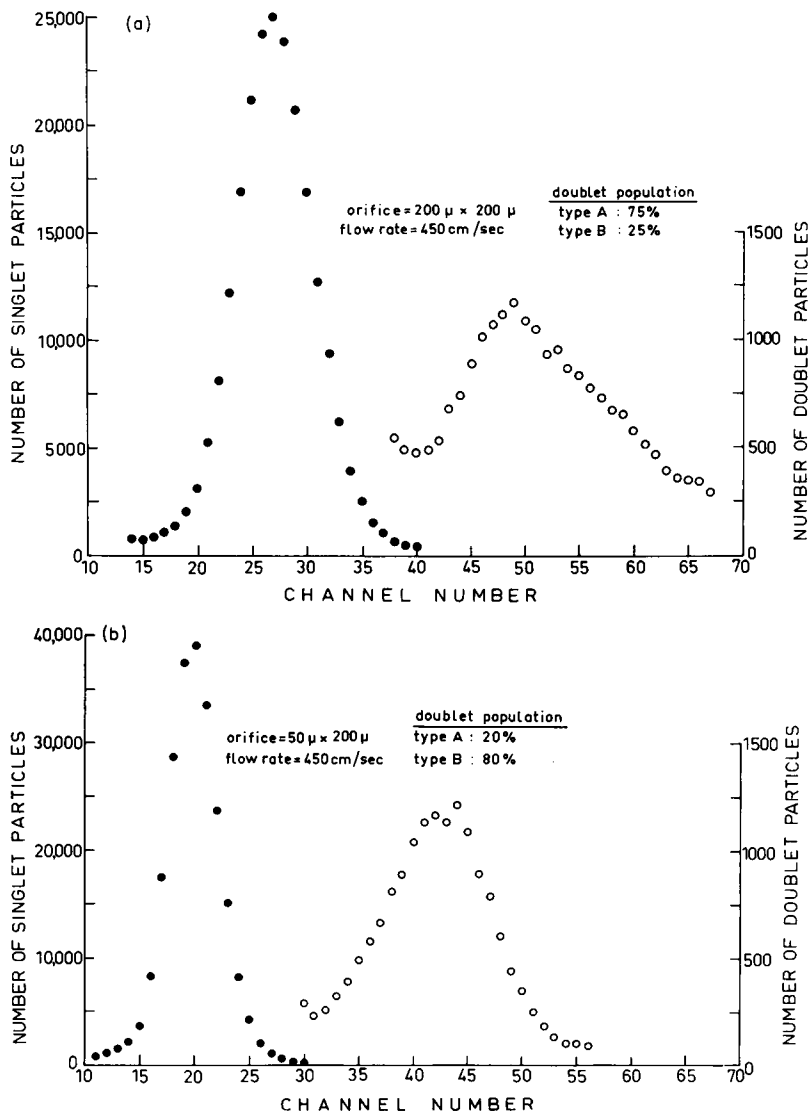
FIGURE 4 Size distribution of singlet (closed circles, left-hand scale) and doublet (open circles, right-hand scale) ragweed pollen particles. The proportion of type *A* and type *B* pulses is indicated for each orifice.

tions are such that most of the doublets remain in the core region (pulses predominantly type *A*, giving rise to α mode) to somewhat below its maximum $\gamma(b)$ of 1.7 when most of the doublets undergo complete rotation (type *B*, β mode). This is illustrated in Fig. 4.

Fig. 4 *a* is a frequency plot of pulse amplitudes obtained by pumping (450 cm/sec) ragweed pollen particles through an orifice 200 μ in diameter by 200 μ in length

using the measuring system described in detail previously (25). From the ratio of mean doublet channel to mean singlet channel, we obtain a value for γ of 1.41, as expected for the case of normal flow in wide orifices. Note that we have the usual positively skewed distribution, the mean lying to the right of the mode (α mode). If we now use the same flow rate but with a narrower orifice (50 μ), we obtain the plot shown in Fig. 4 b. Here the mean lies to the left of the mode (β mode), and γ has a value of 1.60. It is clear that the change in the hydrodynamic field has resulted in a shift from predominantly (3:1) type A pulses, which produce the α mode, to predominantly (1:4) type B pulses, responsible for the β mode. In fact a much better estimate of γ can be obtained in each case by using the mode channel rather than the mean, since the position of the mode is far less affected by minority-type pulses (even in the presence of overlap between the two distributions). When this is done, we find that γ for the α mode is 1.36 and for the β mode 1.66. In order to improve the lower estimate of γ, the number of type B pulses that contribute to the β population can be decreased by adjusting the gate for minimum width; the α mode then given an apparent γ of 1.26. These results are very close to the predicted values of 1.2 and 1.7, especially when one realizes that because of the actual geometry of the doublet, $\gamma(a)$ should theoretically be slightly higher and $\gamma(b)$ slightly lower than the corresponding parameters in the case of a perfect 2:1 prolate of equal volume.

Anderson and coworkers (27) have briefly reported similar results using synchronized Chinese hamster ovary cells in suspension culture. They studied the size distribution of the parent and daughter cells after mitosis, and their data show that the peak produced by the unseparated daughter cells is positively skewed and with a shape factor as calculated from the α mode of 1.23. This is in even closer agreement with the expected value of 1.21, probably because undissociated cell pairs approximate the theoretical shape of a 2:1 prolate spheroid much better than do rigid tangent spheres.

An additional correction must be made to account for the fact that the particle diameter is not always negligible compared with the orifice diameter. The previous treatment (24), which tended to underestimate the correction, was based on results derived from close-packing models and assumed that the orifice and particle were geometrically similar in shape. Since this is strictly true only for cylindrical particles, a spheroidal particle in a cylindrical orifice must be handled differently. Unfortunately such mixed boundary problems are difficult to solve, even numerically, and solutions have been published for only a few special cases (28, 29). Smythe (28) has evaluated γ for four different spheroids, and his calculations predict a shape factor increase in the 50 μ orifice of slightly over 5 % for the ragweed sphere and under 8 % for the 2:1 prolate. The latter increase refers to $\gamma(a)$, and although the corresponding increase in $\gamma(b)$ was not determined, one would expect it to be even higher. Thus γ as derived from the ratio of mode doublet channel to mode singlet channel is too high in the 50 μ orifice by about 2 % in the case of $\gamma(a)$ and by somewhat more in the case of $\gamma(b)$. Doubling the orifice diameter decreases the correction

by a factor of approximately eight. [Note that the formal application of Smythe's results requires that all the spheroids be measured while lying along the orifice axis; in practice, the migration of particles towards the core region that takes place (24) at large particle-diameter/orifice-diameter ratios is usually sufficient to satisfy this condition.]

Experimentally, any overlap between the α and β distributions will, of course, tend to increase the discrepancy for both $\gamma(a)$ and $\gamma(b)$. Table I contains values of γ determined from experimental data on four different orifices as explained above, but without the Smythe correction. Because the comparison is made at constant fluid velocity, the relevant parameter in the characterization of the hydrodynamic field (24) is L/R^2, and so it too is listed in the table. (When the Reynolds number is held fixed instead, the relevant parameter becomes L/R.) The skew has been calculated according to Pearson as mean value less modal value, in units of standard deviation. Theoretical limitations on the minimum permissible length of an orifice of a given radius (24) preclude any attempt to approach $\gamma(a)$ more closely in this system; with oblate spheroids the situation is much more favorable. Thus a prominent α or β mode provides a very accurate measure of the axial ratio of a spheroid of known volume; conversely, equally accurate mean volumes can be obtained if particle shape is known. This, despite the simplifying assumptions used to arrive at our description of the hydrodynamic field and the lack of a precisely quantified mechanism of rotation.

From the theoretical expressions presented previously (24), it is easily seen that the ratio of minimum shape factor to maximum shape factor, $\gamma(a)/\gamma(b)$, is always independent of the volume of the particle and is, in fact, just $\gamma(a) - \frac{1}{2}$ for a prolate spheroid and $2\gamma(a) - 2$ for an oblate. It is thus possible to determine both the volume of the particle and its minimum shape factor (and axial ratio) by choosing the experimental conditions such that in one case the α mode is dominant and in the other case the β mode is dominant; the accuracy of any such determination will depend on the extent to which these extremes can be approached. If the spheroids

TABLE I

PARAMETERS OF RAGWEED POLLEN PARTICLE DOUBLET DISTRIBUTIONS IN VARIOUS ORIFICES AT FLOW RATE OF 450 cm/sec

Orifice dimensions (nominal)			Results		
Length L	Radius R	Ratio L/R^2	Mean γ	Mode γ	Skew
μ	μ	μ^{-1}			
200	100	0.02	1.407	1.358*	+0.302
400	100	0.04	1.467	1.442	+0.163
300	50	0.12	1.528	1.577	−0.273
200	25	0.32	1.600	1.662	−0.322

* This value can be decreased to 1.26 by adjusting the gating circuits for minimum width.

undergo only partial deflection rather than complete rotation when they enter the boundary layer, or if their major axes are not completely aligned parallel to the orifice axis, there will be an underestimation of the eccentricity of the particle and hence of its volume; the presence of any overlap between the α and β distributions will have a similar effect, though smaller.

RED BLOOD CELLS

Having explained the behavior of our model particles, we now turn to a considera tion of red blood cells. Human red blood cells were prepared in the usual way (see, for example, reference 10) and suspended in isotonic phosphate-buffered saline. Fig. 5 illustrates typical type A and type B pulses obtained in an orifice 50 by 150 μ under normal experimental conditions (orifice current, 170 μamp; flow rate, 450 cm/sec). Like the ragweed doublets (cf. Fig. 2), the red cells enter the orifice with their minor axes in a plane perpendicular to the axis of the orifice; some of them traverse it entirely within the core region (type A), others (type B) enter the boundary layer and are deflected. A characteristic of red blood cell pulses that is absent in the case of the rigid ragweed is the variable peak height of the type B pulses (Fig. 5 d). This variation indicates that the cells are not rotated completely by the gradient across the edge of the boundary layer, as we suggested may occur for oblate spheroids of such eccentricity, or that they undergo distortion, or both. If the red cells are not distorted, then increasing the flow rate should not only decrease the relative number of type B pulses, as before, but should also shift the β mode to the right. To see whether this actually does take place, a series of measurements was carried out at different flow rates; the results are shown in Fig. 6, which includes contours of the core regions and the relative proportions of type A and type B pulses. The hydro-dynamic field can be seen to have a considerable effect on the distribution pattern, the familiar positive skew (a dominant α mode with little overlap) being obtained at intermediate flow rates only. (Unlike with ragweed, here the electric field does does have an effect under certain conditions, see below.) At extreme flow rates (both high and low) the proportion of type B pulses appears to decrease and the position of the β mode shifts to the left, causing the height of the α mode to increase and the skew to decrease; the position of the α mode, however, remains unchanged. Such complex behavior forces us to abandon our analogy with the rigid ragweed doublets and ascribe the shape of type B pulses in red blood cells to the combined effects of deflection and distortion. This will be discussed further in the next section, but it is already clear that the α mode provides a much better estimate of $\gamma(a)$ than the β mode does of $\gamma(b)$, and in what follows we shall determine the axial ratio of the red blood cells from the α mode and $\gamma(a)$.

A large number of experiments using blood from different healthy adults was carried out in an orifice 50 by 100 μ at a flow rate of 450 cm/sec. These conditions were chosen in order to decrease the number of type B pulses and provide a promi-
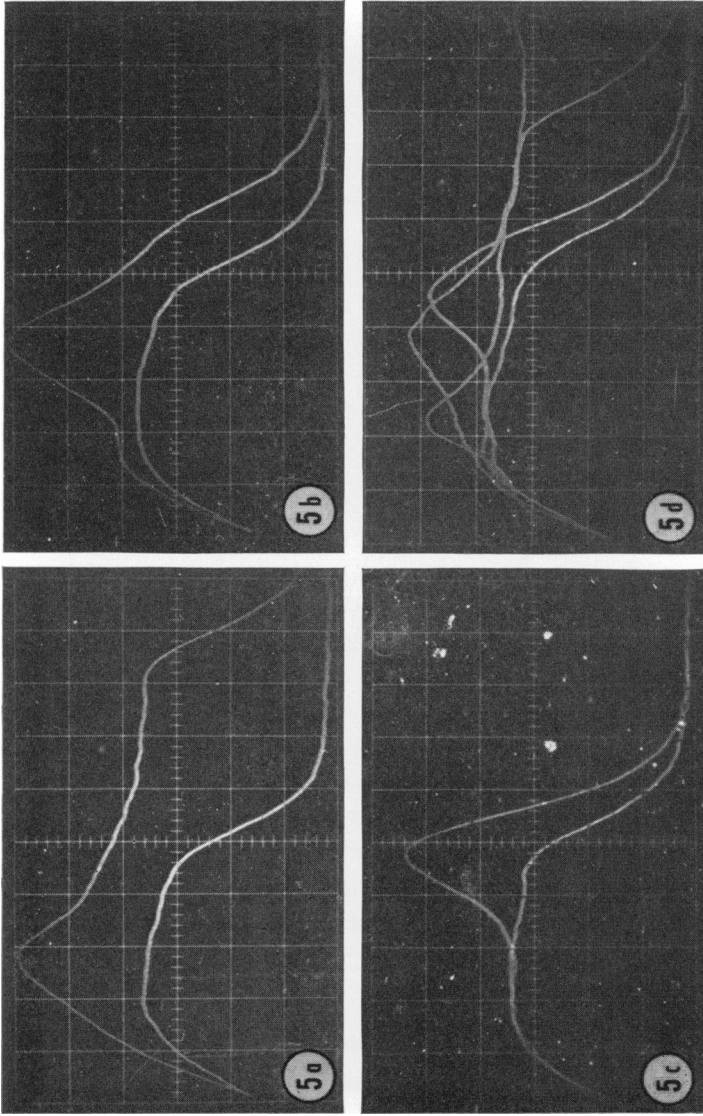
Figure 5 Oscillograms of pulse shapes of human red blood cells in an orifice 50 × 150 μ. Flow rate, 450 cm/sec; current, 170 μamp; sweep, 5.0 μsec/division.
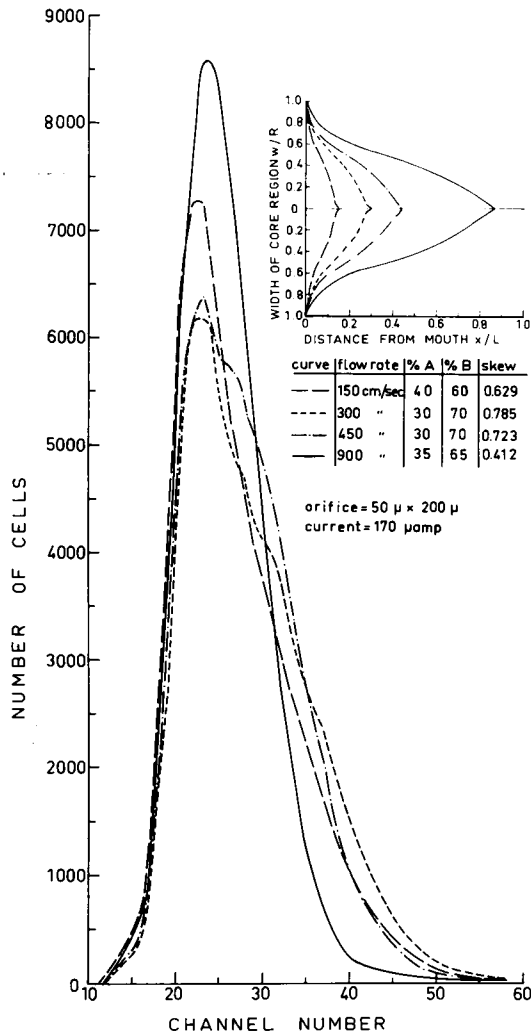
FIGURE 6 Size distribution of human red blood cells. *Inset*: Contour of width of core region *w* in units of orifice radius *R* as a function of distance from mouth of orifice *x* in units of orifice length *L*. The proportion of type *A* and type *B* pulses and the skew are indicated for each flow rate.

nent α mode with little overlap; the cell-diameter/orifice-diameter ratio here is small enough to make the correction negligible ($< \frac{1}{2}\%$). The modal size (shape factor $\times$ volume, for a nonconducting particle) of 10 different samples of cells was found from their α mode to average 102.7 μ^3 with a coefficient of variation of 1.8%. Using the accepted value of 87 μ^3 for the mean cellular volume of red blood cells (30), we obtain a shape factor for the α mode of 1.18 which, for a perfect oblate spheroid, corresponds (24) to an axial ratio of 0.26 and a major axis of 8.6 μ. This is in very

good agreement with the known dimensions of these cells in isotonic media (31), and suggests that here, too, our description of what takes place during passage through the orifice is essentially correct. (By comparison, if we take the mean size rather than the α mode, we get an axial ratio of 0.62!) In addition it follows that, unlike the cells that leave the core region, those that give rise to the α mode preserve their original shape while in the orifice and are not distorted.

This agreement also implies something else: equality between the *mean* volume, on which the value quoted from the literature is based, and the volume derived from the *modal* size, on which our results are based. If the shape factor is not a strong function of volume, then it follows that the volume distribution of red blood cells is unskewed (in the pearsonian sense), and so it may be possible to fit it to one of the known symmetrical distributions. Such is indeed the case, a very satisfactory fit being obtained with the normal (gaussian) distribution.

In order to test the goodness of fit of the distribution $n(x)$ of cells per channel (or per unit size or per unit volume), one takes the position of the α mode (interpolating between channels, if necessary) as the modal channel x and calculates the total number of cells N and their standard deviation σ by using the values of $x \leq x$ and assuming symmetry of $n(x)$ about the mean (mode). Typical results are shown in Fig. 7 for an orifice 50 by 100 μ and a flow rate of 450 cm/sec. The histogram represents experimental data, the solid line is a theoretical curve of a normal distribution, with parameters obtained as discussed above. A χ^2 analysis in the region to the left of the α mode $(x \leq x)$ gives a probability of greater than 90% for the occurrence of random deviations between the two distributions to be as large as those obtained, a not at all unlikely event, and we conclude that the size [and hence volume, pro-
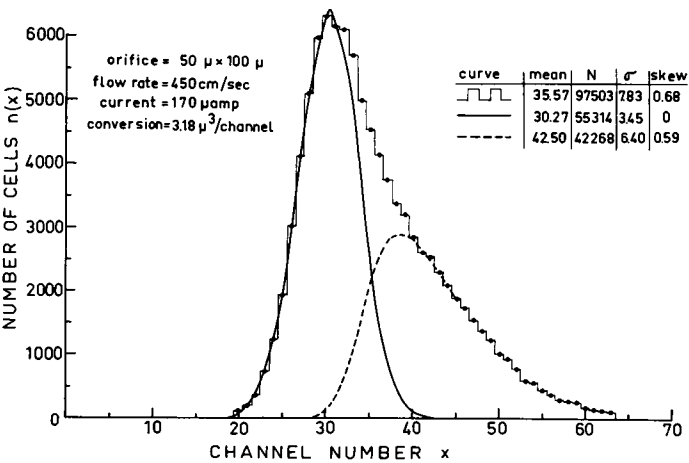

FIGURE 7 Size distribution histogram (experimental points) of human red blood cells. Solid curve represents calculated normal distribution for α population, dashed curve is β population obtained by subtraction.

vided that $\gamma(a)$ is reasonably uniform throughout the population] of human red blood cells is a normally distributed variable.

The distribution of the α population to the left of its mode having been established, we can now rely on symmetry to complete the distribution to the right and reconstruct the β population by subtraction. This is shown by the dashed curve in Fig. 7. Incidentally, the β population is not normally distributed ($P \ll 1\%$), as expected if different cells undergo different degrees of deflection and distortion as they enter the boundary layer.

In the event that the extent of the overlap between the α and β populations (or the presence of noise) makes the determination of N and σ unreliable even in the region to the left of the α mode, accurate estimates of these parameters can readily be obtained, provided only that $\bar{x}$ is known by fitting a regression line (a least squares fit) to $\ln n(x)$ as a function of $(x - \bar{x})^2$: the slope is just $-\frac{1}{2}\sigma^2$ and the value of $n(x)$ at the intercept $(x = \bar{x})$ is $N/\sigma(2\pi)^{1/2}$. Overlap will cause the larger values of $\ln n(x)$ to be somewhat high while noise will increase the smaller values; the actual experimental conditions should dictate the best range to select for the fit. For the data of Fig. 7, the use of this least squares N and σ improves the normal distribution fit to $P > 95\%$.

It has been noted above that not only the hydrodynamic field, as in the case of the ragweed doublets, but also the electric field can alter the degree of overlap between the α and β populations. The effect of electric fields on the size of cells will be treated in detail in a subsequent paper in this series; we mention here only the results relevant to the present discussion.

There exists a certain critical electric field E_c above which the size (*not* volume) of the cells decreases for increasing field E. The value of E_c lies in the vicinity of 0.8 kv/cm for human red blood cells in isotonic phosphate-buffered saline, and is independent of orifice dimensions and current. For $E > E_c$, both the α mode and the β mode decrease; since the former does so more than the latter, the separation between them actually increases with increasing field. All the data on red blood cells reported in this paper have been obtained at fields below E_c.

DISCUSSION

In order to be able to interpret the experimental data on the size distribution of red blood cells, we first found it necessary to investigate the behavior of rigid spheroids possessing a well-defined shape and volume. Ragweed pollen particles were chosen for this purpose because they are uniform, nonconducting, rigid spheres (25) that are readily prepared in suspensions containing both single particles and spherical doublets; these doublets all have the same shape (tangent spheres of equal size), and their mean volume is just twice that of the single spheres.

By observing the electrical signals produced during the passage of these doublets through the orifice and associating them with the resulting size distribution histo-

grams under various experimental conditions, we arrived at a semiquantitative model involving the hydrodynamic forces within the orifice that was able to account for the data and to predict in large measure the behavior of red blood cells. In particular, and much to our good fortune, it was found that all the ragweed doublets enter the orifice with their major axes aligned parallel to the orifice axis. Some of them maintain this orientation during their passage through the orifice, giving rise to flat-top pulses, while others are rotated and produce pulses with peaks (Fig. 2). The reason for the peak is that the amplitude of the signal produced by a particle within the orifice is proportional to the product of its volume v and its shape factor γ. This shape factor is a function of the orientation of the particle, being a minimum $\gamma(a)$ for any particular spheroid when its major axis lies parallel to the electric field (orifice axis) and a maximum $\gamma(b)$ when its minor axis is parallel. Thus all ragweed doublets enter with minimum shape factor $\gamma(a)$; those that pass through that way produce the flat pulses while the others, which are rotated during passage, undergo a rise in shape factor to $\gamma(b)$ which then returns to $\gamma(a)$ as the 180° rotation is completed. This produces pulses containing a peak, and since the usual detection circuits (25) measure peak values, the size (γv) distribution histogram that results from such a measurement will depend on the values of $\gamma(a)$ and $\gamma(b)$ and on the proportion of particles that undergo rotation. Both shape factors are fully determined by the axial ratio of the spheroid (24), whereas the number of doublets that are rotated depends strongly on the hydrodynamic field. This is readily demonstrated by performing two experiments under the same conditions but using orifices of different diameters; with the wider orifice most of the pulses (75%) are flat while with the narrower one most of them (80%) are peaked. The size distribution histograms that result (Fig. 4) can be explained on this basis alone, and are taken as confirmation of our interpretation of size distribution in terms of particle orientation by the hydrodynamic field.

It should perhaps be mentioned that the particles (and cells) that give rise to the peaked pulses have periods of rotation near what is to be expected for spheroids in shear flow (24, 32) but, unlike the theoretical predictions, they do not rotate through more than 180° (Figs. 2 and 5).

Turning to the more complex problem of red blood cells, we found that they too all enter the orifice with their minor axes perpendicular, some passing through with rotation and some without. But red blood cells differ from ragweed doublet particles in two important respects: they are not (necessarily) rigid, and they approximate oblate rather than prolate spheroids. As oblates the requirement that their minor axes on entrance be perpendicular to the orifice axis is sufficient to define their shape factor uniquely, $\gamma(a)$, but not their orientation, and any position between the two extremes illustrated in Fig. 8 (a, d) may occur. [Note that the third extreme (c) as well as positions intermediate between it and both (a) and (d) have been shown not to occur.] When the cells leave the core region and enter the boundary layer, those (d) with their equatorial plane oriented along a radius of the orifice will be rotated
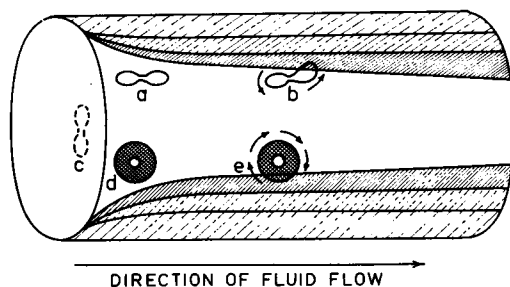
DIRECTION OF FLUID FLOW

FIGURE 8 Schematic representation of possible extreme red blood cell orientations within an orifice before (a, d) and after (b, e) entering boundary layer (hatched). Arrows indicate direction of rotational forces. Not to scale. (Orientation c has been shown not to occur.)

(e) by the hydrodynamic field about their axes of symmetry while the others (a) will tend to rotate (b) about a major axis. Thus the former do not undergo any change in shape factor during passage and so produce a flat-top pulse; this is the reason that not all the pulses are peaked despite the fact that the contours of the core regions indicate that all the cells are rotated (Fig. 6). Those cells (a) with their equatorial plane perpendicular to a radius, on the other hand, will experience the hydrodynamic shear across their smallest dimension (b), and when these forces become large enough to overcome the rigidity of the cells, they will bend under the stress. Raising the flow rate would merely increase the extent of the bending and so decrease the shape factor and hence the skew of the size distribution. Another possible factor contributing to this decrease and to the slight decrease in the proportion of type B pulses could be the lowering of part of the contour profile that takes place at higher flow rates; because there the component of the gradient in the direction of rotation actually decreases with increasing flow rate, the forces in that region may become too small to deflect the cells at all. At low flow rates, of course, there will be no distortion, and the deflection caused by the gradient will be much less. Thus the decrease in the proportion of type B pulses and in the skew that is seen in Fig. 6 can be explained for the high flow rate as well as for the low, but in a very different way.

In general one can say that the β mode for nonrigid particles may reflect a shape factor that is much less than γ (b) and should not be used to calculate particle shape or volume without first establishing its reliability in each individual case; $\gamma(a)$, on the other hand, can be used with confidence. For rigid particles both $\gamma(a)$ and $\gamma(b)$ are dependable, so that by choosing the experimental conditions such that first the one and then the other is measured, both the mean volume of a population of particles and their shape can be obtained without recourse to independent data (provided that the axial ratio is reasonably uniform throughout the population).

The possibility that the orientation of a red blood cell within the orifice can affect the magnitude of the electrical signal which it generates was first suggested by Gutmann (17), but he assumed that this was the origin of the M-shaped pulses he observed and that these pulses were the cause of the skew in the red cell size distribu-

tion. Thom and coworkers (18) made a more thorough investigation of red blood cell sizing and considered nonuniform electric fields, cell shape, and cell deformation. They realized, as we have already shown (24), that the M-shaped pulses result from the higher electric field near the walls of the orifice, and they attributed the skewed distribution to them; it is clear from the present study, however, that the skew is actually caused by particle rotation in the boundary layer. This possibility was raised by Shank et al. (15) who, like the other group, designed a mechanical device to confine the flow of cells to a narrow region about the orifice axis. When orifice dimensions and flow rates are suitably chosen, we can expect such a device to eliminate both the M-shaped pulses and particle rotation, and so produce the symmetrical distributions reported, but exactly what else it does has yet to be established. Thom and coworkers (18) concluded that because of the large hydrodynamic forces at the entrance of the orifice, all red blood cells become deformed into prolate spheroids and their shape factors approach unity; similar conclusions, although more qualitative in nature, were arrived at by Shank et al. (15). It may well be that with capillary-directed flow all the cells are indeed deformed as suggested, but our analysis of pulse shapes makes it quite clear that under normal experimental conditions the red blood cells enter the orifice as undeformed, oblate spheroids: some of them pass through it entirely within the core region and so remain that way while the others cross into the boundary layer and are rotated, being either deformed in the process or not, depending on their orientation.

The mean size (shape factor $\times$ volume) of the red blood cells of 10 healthy adults was found to be 102.7 μ^3 with a coefficient of variation for the samples of 1.8%, Substituting for the mean cellular volume (87 μ^3), one obtains a shape factor of 1.18, corresponding (24) to an axial ratio of 0.26. This is quite close to the accepted value (31), and since axial ratio is a sensitive function of shape factor (24), it implies that 1.18 is a very accurate result. (Actually the value 1.18 represents the mean shape factor weighted according to cell volume, but unless the shape factor shows a marked dependence on volume, such a weighting will not have much effect.) The value 0.26 was obtained by assuming that the red blood cell is a perfect oblate spheroid, which it is not, and since the relationship between shape factor and axial ratio depends on the precise geometrical form of the red blood cell, it is difficult to estimate the error that such an approximation entails. An axial ratio of 0.26 in a spheroid of 87 μ^3 fixes the major axis at 8.6 μ, in excellent agreement (1%) with the accepted value for the equatorial diameter of the red blood cell (31). Nevertheless, owing to the geometrical idealization involved, these axial dimensions are better thought of as describing an electrically equivalent oblate spheroid rather than the red blood cell itself.

The fact that the size of red blood cells is normally distributed is very convenient because it facilitates comparisons among cell populations, but when the cells are derived from animals in different physiological or pathological conditions, it must first be demonstrated experimentally in each particular case that such cells can be sized the same way as are normal red blood cells, by their α mode. And while cell

size is a normally distributed variable, it does not necessarily follow that cell volume is normally distributed; it all depends on the relationship between the shape factor of a cell and its volume.

REFERENCES

1. PRICE-JONES, C. 1922. *J. Pathol. Bacteriol.* **25**:487.
2. MATTERN, C. F. T., F. S. BRACKETT, and B. J. OLSON. 1957. *J. Appl. Physiol.* **10**:56.
3. GRANT, J. L., M. C. BRITTON, JR., and T. E. KURTZ. 1960. *Am. J. Clin. Pathol.* **33**:138.
4. WINTER, H., and R. P. SHEARD. 1965. *Aust. J. Exp. Biol. Med. Sci.* **43**:687.
5. JACOBI, H., A. HANSTEIN, W. HANSTEIN, and W. KÜNZER. 1967. *Klin. Wochenschr.* **45**:154.
6. BRECHER, G., E. F. JAKOBEK, M. A. SCHNEIDERMAN, G. Z. WILLIAMS, and P. J. SCHMIDT. 1962. *Ann. N. Y. Acad. Sci.* **99**:242.
7. LUSHBAUGH, C. C., N. J. BASMANN, and B. GLASCOCK. 1962. *Blood.* **20**:241.
8. LUSHBAUGH, C. C., N. J. BASMANN, and D. B. HALE. 1963. *In* Biological and Medical Research Group (H-4). The Health Division of Los Alamos Scientific Laboratory, Los Alamos, New Mexico. U. S. Atomic Energy Commission Report LA-3034-MS. 261.
9. LUSHBAUGH, C. C., and D. B. LUSHBAUGH. 1965. *South. Med. J.* **58**:1208.
10. DOLJANSKI, F., G. ZAJICEK, and J. NAAMAN. 1966. *Life Sci.* **5**:2095.
11. UR, A., and C. C. LUSHBAUGH. 1968. *Br. J. Haematol.* **15**:527.
12. VAN DILLA, M. A., N. J. BASMANN, and M. J. FULWYLER. 1964. *In* Biological and Medical Research Group (H-4). The Health Division of Los Alamos Scientific Laboratory, Los Alamos, New Mexico. U. S. Atomic Energy Commission Report LA-3132-MS. 182.
13. WECHSELBERGER, E. 1970. *Blut Z. Gesamte Blutforsch.* **20**:112.
14. BULL, B. S. 1968. *Blood.* **31**:503.
15. SHANK, B. B., R. B. ADAMS, K. D. STEIDLEY, and J. R. MURPHY. 1969. *J. Lab. Clin. Med.* **74**:630.
16. VAN DILLA, M. A., N. J. BASMANN, and M. J. FULWYLER. 1964. *In* Biological and Medical Research Group (H-4). The Health Division of Los Alamos Scientific Laboratory, Los Alamos, New Mexico. U. S. Atomic Energy Commission Report LA-3132-MS. 197.
17. GUTMANN, J. 1966. *Elektromedizin.* **11**:62.
18. THOM, R., A. HAMPE, and G. SAUERBREY. 1969. *Z. Gesamte Exp. Med.* **151**:331.
19. WEED, R. I., and A. J. BOWDLER. 1967. *Blood.* **29**:297.
20. LUSHBAUGH, C. C., N. J. BASMANN, and H. ISRAEL. 1962. *In* Biological and Medical Research Group (H-4). The Health Division of Los Alamos Scientific Laboratory, Los Alamos, New Mexico. U. S. Atomic Energy Commission Report LA-2780-MS. 198.
21. LUSHBAUGH, C. C., and D. B. HALE. 1963. *In* Biological and Medical Research Group (H-4). The Health Division of Los Alamos Scientific Laboratory, Los Alamos, New Mexico. U. S. Atomic Energy Commission Report LA-3034-MS. 270.
22. COOPERSMITH, A., and M. INGRAM. 1968. *Am. J. Physiol.* **215**:1276.
23. COOPERSMITH, A., and M. INGRAM. 1969. *Am. J. Physiol.* **216**:473.
24. GROVER, N. B., J. NAAMAN, S. BEN-SASSON, and F. DOLJANSKI. 1969. *Biophys. J.* **9**:1398.
25. GROVER, N. B., J. NAAMAN, S. BEN-SASSON, F. DOLJANSKI, and E. NADAV. 1969. *Biophys. J.* **9**:1415.
26. CARSLAW, H. S., and J. C. JAEGER. 1959. *In* Conduction of Heat in Solids. The Oxford University Press, London. 2nd edition. 46.
27. ANDERSON, E. C., D. F. PETERSEN, and R. A. TOBEY. 1967. *Biophys. J.* **7**:975.
28. SMYTHE, W. R. 1964. *Phys. Fluids.* **7**:633.
29. CHANG, I. C., and I. D. CHANG. 1970. *J. Appl. Phys.* **41**:1967.
30. WINTROBE, M. M. 1967. *In* Clinical Hematology. Lea and Febiger, Philadelphia. 6th edition. 86.
31. PONDER, E. 1948. *In* Hemolysis and Related Phenomena. Grune and Stratton, New York. 14.
32. GOLDSMITH, H. L. 1968. *J. Gen. Physiol. Suppl.* **52**:5 s.